MACHINE-LEARNING BASED THERMAL CONDUCTIVITY PREDICTION OF PROPYLENE GLYCOL SOLUTIONS: REAL TIME HEAT PROPAGATION APPROACH

Andrew JARRETT[1], Ashwin KODIBAGKAR[2], Dugan UM[3], Denise P. SIMMONS[1], Tae-Youl CHOI[1*]

[1]Department of Mechanical Engineering, The University of North Texas, Denton, Texas 76207, USA
[2]School for the Talented and Gifted at Yvonne A. Ewell Townview Center, Dallas, TX 75203, USA
[3] Department of Engineering, Texas A&M Corpus Christi, Corpus Christi, TX 78412, USA
*Tae-youl.choi@unt.edu

The objective of this paper is to evaluate the capability of an Artificial Neural Network to classify the thermal conductivity of water-glycol mixture in various concentrations. Massive training/validation/test temperature data were created by using a COMSOL model for geometry including a micropipette thermal sensor in an infinite media (i.e., water-glycol mixture) where a 500 μs laser pulse is irradiated at the tip. The randomly generated temporal profile of the temperature dataset was then fed into a trained ANN to classify the thermal conductivity of the mixtures, whose value would be used to distinguish the glycol concentration at a sensitivity of 0.2% concentration with an accuracy of 96.5%. Training of the ANN yielded an overall classification accuracy of 99.99% after 108 epochs.

Key Words: Artificial Neural Networks, Classification, Temperature Profiles, Thermal Conductivity, Heat Transfer

1. Introduction

Single-cell thermal properties are a rapidly growing field of study because the thermal energy inside of the cell interacts with all its biochemical reactions [1, 2]. One of the most essential of these properties is thermal conductivity as it governs every heat transfer problem in biomedical engineering. In regards to biology, thermal conductivity can be used as a way to evaluate cell viability and cancerous disease state, similar to the proliferation index in which tumor progression is assessed [3, 4]. Many methods for cellular level thermometry have been created for the measurement of single cells, such as utilizing electron spin from nitrogen vacancies in diamond nanoparticles and fluorescent nanothermometers utilizing nanoparticles [5, 6]. It has been shown that a simple method for single-cell measurement was a combination of a thermocouple inside of a micropipette and laser point heating [7]. Thermal conductivity can then be found from the transient temperature profiles using a COMSOL computational model and a multi-parameter fitting program [8]. However, the process of obtaining the thermal conductivity based on a measured temperature profile was revealed as costly due to large computational time and limited computer resources. Machine learning serves as an efficient alternative to numerical analysis [9].

Machine learning makes it possible to process large amounts of data to accomplish specific tasks, namely, to recognize patterns in the dataset [10]. This is useful in applications such as computer vision, speech processing, and game playing. [11] Artificial Neural Networks (ANN) work on pattern recognition and

are trained with large data sets of known solutions [12]. Once the training is completed, the trained ANN can solve complex problems instantaneously with high accuracy [13]. This is based upon the concept of neurons in the brain, where nodes are connected to synapses with weighted values to make decisions [14]. Many ANNs use supervised training where the error from the known solutions is backpropagated through the system of neurons and the weights are adjusted by the errors between ground truth and ANN outcomes [15]. This process is iterated until an acceptable level of error is achieved [16].

According to recent research reports, the ANN predictive models show a trend that their prediction accuracy is very much affected by ANN structures, used parameters, and the utilized algorithm [17]. Material design through ANN modeling was suggested where an ANN predictive model so-called 'co-training style semi-supervised ANN model' was used to take advantage of unlabeled data to refine the prediction [18]. Machine learning, especially ANN have been used for various thermal characterization related tasks, including the prediction of hybrid nanofluids and ethylene glycol thermal conductivities [19, 20]. These utilize a multi-input single output regression learning model, where the inputs are the concentration, density, and temperature of the fluids. The output is the thermal conductivity of the fluid. Furthermore, ANN modeling has been employed to predict thermal properties of various materials including polymer composites [21], bakery products [22], soils [23], fruits and vegetables [24], rocks [25] and phase change materials [26].

Unlike the Fourier series approach in [20], we propose a real-time approach for the thermal conductivity prediction of a glycol solution by measuring the time-series heat propagation profile. Therefore, an ANN trained with the time-series temperature profiles of known thermal conductivities can be proposed to predict parameters (i.e., thermal conductivity) of a target chemical or a biological system including liquid or a biological cell. To that end, we first obtain massive heat propagation profiles using the partial differential eq. (1) varying the thermal conductivity and training an ANN model for the Sim-to-Real approach. Once trained, classification is instantaneous thereby solving the issues of computation time. Since the AI model is trained by the time-series heat propagation data, the proposed approach is unique and useful for real-time physical and biological property measurement for time-critical medical applications, in-situ biological screening, or real-time physiological metabolism analysis.

In order to obtain a large enough data set for training, a simulation model can be created in COMSOL to create transient temperature profiles of liquids with varying thermal properties. When training is complete, the ANN can be verified with real liquids. This is known as a sim-to-real approach, whereby the network is trained with a simulation dataset from a model and tested with experimental data [19]. This work is intended to show the capability of ANN in classifying the thermal conductivities of a model system (liquid) before this approach is used in sim-to-real cases. Furthermore, this sim-to-real approach as a next step will be utilized in classifying cell or tissue thermal conductivities in *in vivo* setting.

2. Methodology

This section will cover the preparation of the training data, details of the simulation, as well as the method used to structure and train the neural network.

2.1. Training Data Preparation:

Training data were generated using a Partial Differential Equation (PDE) solver. COMSOL Multiphysics was chosen to calculate transient temperature profiles given a parameter – thermal conductivity for a model shown in fig. (1). Thermal conductivity (k) of the PDE in eq. (1) below is the only parameter we used to evaluate the proposed ANN in terms of feasibility in the prediction of thermal conductivity:

$$\rho c_p \frac{\partial T}{\partial t} + \nabla \cdot (-k \nabla T) = Q \tag{1}$$

where ρ is density, c_p is specific heat, T is the temperature, and Q is the heat source at the tip.

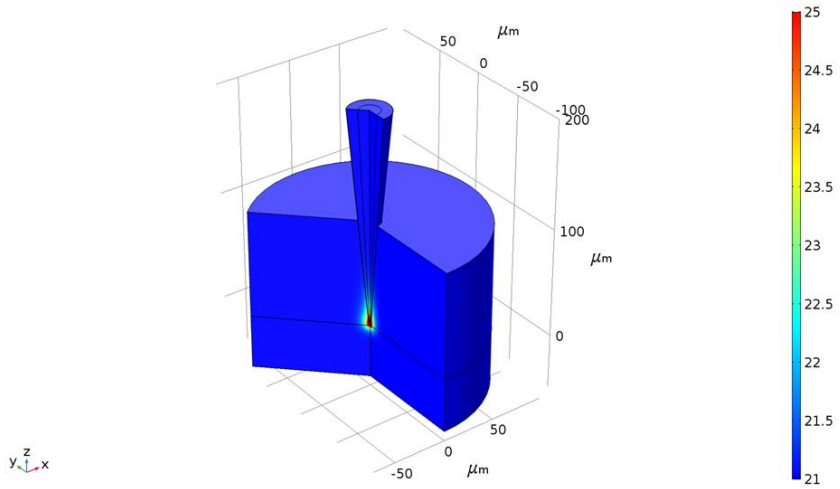

Figure 1: *3D cut away COMSOL Multiphysics simulation of MTS with temperature scale [30]*

The model (Figure 1) represents a micropipette thermal sensor (MTS) subjected to point-source heating at the tip of the sensor. The junction of the thermocouple (i.e., MTS) is an inner core of bismuth and a thin outer coating of nickel with a 200 nm thickness. The simulation was built by a 2D axisymmetric model of the MTS surrounded by a cylindrical fluid domain, with radius of 100 µm and height of 150 µm. In the simulation, a fine mesh was selected where element sizes range from 13.3 - .75 µm. The size on the mesh was decided by comparing the temperature profiles from 4 different sizes (13.3, 9.26, 5.0, and 2.5 µm), it was found that there was only an RMS Error value of .01103 K between a mesh size of 13.3 and 2.5 µm. Therefore, the fine mesh size of 13.3 was used to save on computational time. On the outer nickel coating of the micropipette, a boundary layer was selected to increase the density of the mesh, for enhanced accuracy of the conduction. The boundary condition for this study was setting the change in heat on the outer edge of computational domain to zero. This boundary condition signifies no heat transfer at the edge of the boundary during the time of short heat pulse of 500 µs. COMSOL performed a time dependent temperature direct solution using the PARDISO method [27].

The evolution of temperature depends upon the thermal conductivity of the surrounding liquid – water and glycol mixture in the current study. A 100 µW single-shot point heat source with a Gaussian profile and a 500 µs pulse duration was set on the center of the MTS tip. The temperature profile was taken from

the surrounding liquid and saved for the training data set. The accuracy of the numerical model was verified by experimental cross check from our previous paper [8]. In this report, the same numerical model was used to calculate the transient temperature evolution to compare it with experimentally measured data to estimate thermal conductivity of various, known non-volatile fluids within 2-3% accuracy.

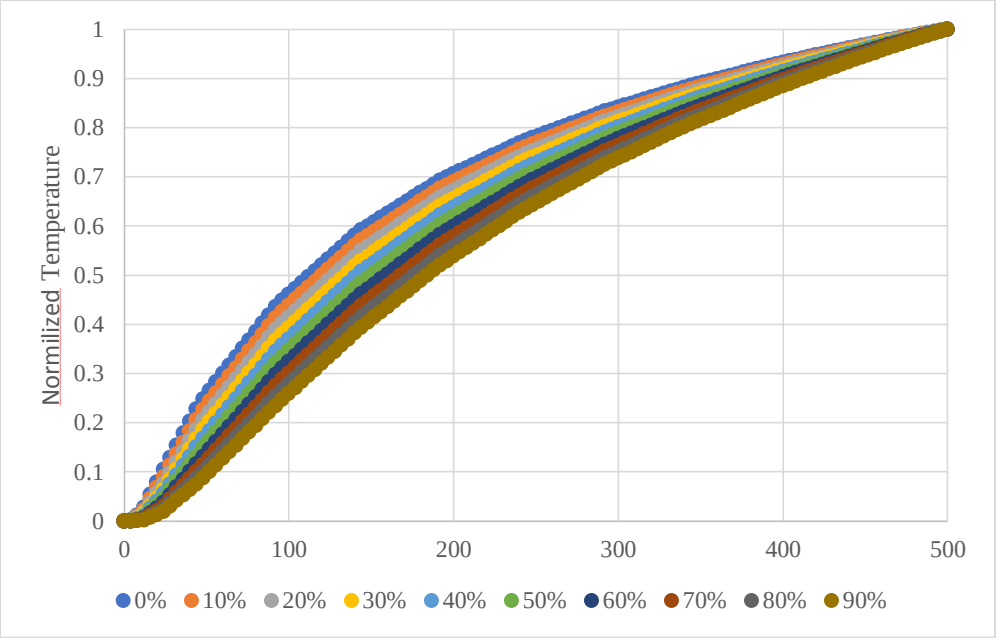

Figure 2: *Normalized temperature profiles of propylene glycol concentrations*

The concentration of glycol in water has a direct impact on the mixture's thermal properties. Specifically, thermal conductivity decreases with the increase of glycol. Differences in thermal conductivity vs. the concentration can be seen in table. (1), which separates the data and assigns each thermal conductivity range a label. Nine different labels were created for 10% changes in glycol concentrations. Next, 100 temperatures vs. time data sets were generated for each of the classification labels, for a total of 900 sets to be used for training the ANN. Each data set had 126 data points to correspond to temperature sampling every 4 µs for a 500 µs duration. This temperature data was normalized using the min-max method [28], which is shown in eq. (2). T_{min} and T_{max} represent the minimum and maximum temperatures of that data set, respectively.

$$T_{Normilized} = \frac{T_i - T_{min}}{T_{max} - T_{min}} \tag{2}$$

Normalization allows for the data to be set on the same scale. This is important in machine learning when the range for the data is different and allows for faster convergence [16]. Along with this faster convergence the magnitude or power of the point heat source becomes negligible, and the profile only depends on the thermal conductivity. These normalized profiles can be seen in Figure 2.

***Table 1**: Range of thermal conductivity values*

Glycol %	Thermal Conductivity Range (W/mK)	Density (Kg/m^3)	Classification Label
0% - 10%	.608 - .542	999.4 - 1009.2	[1 0 0 0 0 0 0 0 0]
10% - 20%	.541 - .484	1009.3 - 1020.1	[0 1 0 0 0 0 0 0 0]
20% - 30%	.483 - 432	1020.2 - 1029.4	[0 0 1 0 0 0 0 0 0]
30% - 40%	.431 - .385	1029.5 - 1037.3	[0 0 0 1 0 0 0 0 0]
40% - 50%	.384 - .342	1037.4 - 1043.9	[0 0 0 0 1 0 0 0 0]
50% - 60%	.341 - .303	1044.0 - 1049.3	[0 0 0 0 0 1 0 0 0]
60% - 70%	.302 - .268	1049.4 – 1053.5	[0 0 0 0 0 0 1 0 0]
70% - 80%	.267 - .238	1053.6 – 1054.2	[0 0 0 0 0 0 0 1 0]
80% - 90%	.237 - .214	1054.3 – 1052.3	[0 0 0 0 0 0 0 0 1]

2.2. Training ANN with simulated data

Once the training data was prepared, a neural network model is designed and trained. The Neural Net Pattern Recognition tool in MATLAB was used to generate and train the designed network using the default scaled conjugate gradient method (SCGM). This method is similar to the gradient descent method where the gradient of the cost function with respect to weights is calculated and subtracted from each weight set to reach a minimum. The difference comes in through the learning rate. In SCGM the learning rate is varied based on the slope of the gradient [29]. Therefore, if the gradient is large, the learning rate increases and decreases if the gradient is small. This allows for faster and more accurate learning when compared to traditional gradient descent in which the learning rate is constant.

The cost function that was used to represent uncertainty in this study is the cross-entropy loss function (CELF) [28]. This loss function is based upon the concept of entropy or the uncertainty in possible outcomes. When the probability of the ANN classifying the correct output is high the loss of the function is minimized.

$$L_{CE} = -\sum_{i=1}^{n} t_i \log(p_i) \quad (3)$$

where *p* and *t* are the probability and true result, respectively.

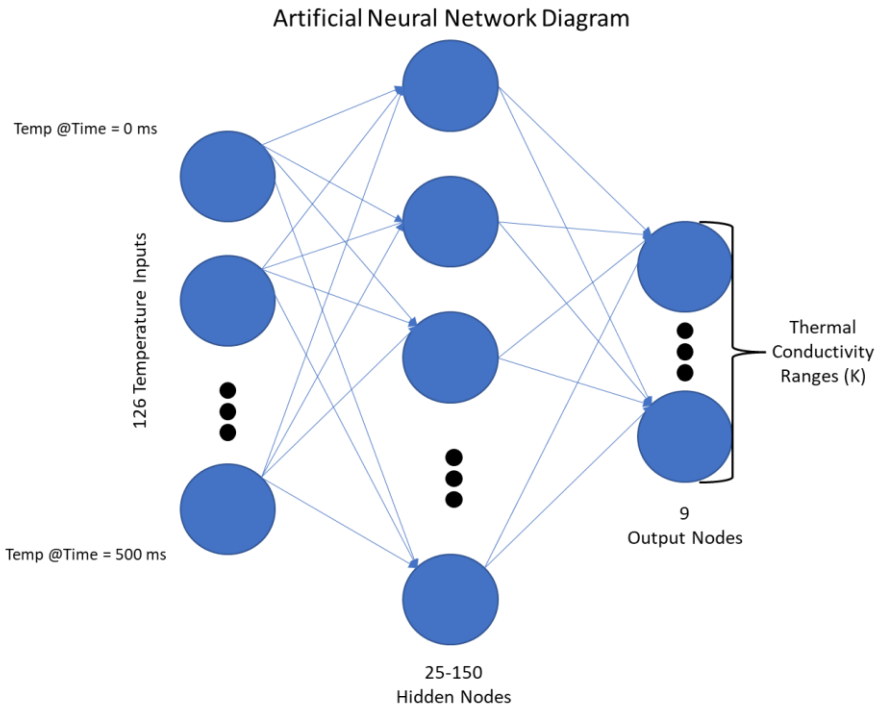

Figure 3: *Neural Network Diagram, left side is the 126 temperature imputes connected by a system of weights to the hidden layer. Lastly, the hidden layer is connected to the output nodes that represent the thermal conductivity ranges.*

A network diagram is shown above in Figure 3. The 126 input nodes correspond to the temperatures at 4 μs time intervals. The differently sized hidden layers were generated from 25 to 150. Next, the output was a vector of 9 nodes to represent the different classification labels. The normalized data were randomized and separated into 70% training, 15% validation, and 15% testing data sets. Training data sets are used with optimization methods such as gradient descent. Validation sets provide a way to evaluate the model during training. This prevents overfitting of the data by early stopping. The final testing data is used to evaluate the trained model.

2.3. Evaluating the Network

The network can be evaluated by using a confusion matrix. This matrix is a visual way to view the performance of the network. It shows the number of true positives (*TP*), true negatives (*TN*), false positives (*FP*), and false negatives (*FN*) produced by the network from the training, validation, and testing data. Most confusion matrixes are shown from binary machine learning models, meaning only two outputs. In this study, the confusion matrix generated is from a multiclass machine learning model, where there were 9 outputs.

There are several metrics that can be utilized to evaluate the performance of a classification mode: Precision, Accuracy, and F1 score [30]. Precision represents the number of positive classifications the

network returned that were positive. Recall indicates the number of positive samples that were correctly classified. The F1 score is the harmonic mean of the precision and recall of the model.

$$Recall = \frac{TP}{TP+FN} \tag{4}$$

$$Precision = \frac{TP}{TP+FP} \tag{5}$$

$$F1\ Score = 2 * \frac{Prcision*Recall}{Precision+Recall} = \left(\frac{2*TP}{2*TP+FP+FN}\right) \tag{6}$$

In the case of the multiclass model, each of the metrics can be found by the individual classification or by the total *TP*, *FP*, and *FN* of the model. When the totals are used to calculate the recall and precision, the following F1 score is known as the micro F1 score. This can be seen eq. (7) where *T.Precision* and *T.Recall* is the total precision and total recall, respectively. In which the total means these are metrics are calculated using *TP* of the entire matrix over the number of data sets used in the matrix, because the *FP* and *FN* are considered equivalent. Therefore, in multiclass models, the accuracy, precision, and micro F1 score are all equal. The macro F1 score can also be used, as it calculates the average of the individual class's F1 score. Therefore, it depends on each class F1 more than the overall accuracy of the network. Lastly, the weighted F1 score can be found by using the total number of samples for each class and multiplying by their F1 score and dividing by the total number of samples.

$$Micro\ F1\ Score = 2 * \frac{T.Precision*T.Recall}{T.Precsion+T.Recall} \tag{7}$$

$$Macro\ F1\ Score = \frac{1}{N}\sum_i^N F1\ Score_i \tag{8}$$

$$Weighted\ F1\ Score = \frac{\sum_i^N (W_i * F1\ Score_i)}{\sum_i^N W_i} \tag{9}$$

3. Results and Discussion

3.1 Training Results for the ANN:

The first part of the study was to determine the number of nodes that would yield the lowest error in classification. Six different networks were created with different hidden layer sizes ranging from 25-150. All networks were given the same simulated data in which each class represent a 10% change in glycol. Next, the micro and macro F1 score was calculated using each network's confusion matrix. Since each class had the same amount of data the Weighted F1 score would be equal to macro F1. The micro and macro F1 scores were almost equal except for the 50-node configuration. This is mostly caused by the lower accuracy of the network and in turn higher deviation between each class F1 score when compared to the other network configurations. Results for this are shown in table (2).

Table 2: *Results of hidden layer size testing from 10% change in glycol concentration where column one represents the hidden layer size, two is the micro F1 score, and three is the macro F1 score*

Hidden Layer Size	Micro F1 Score	Macro F1 Score
25	.9988	.9988
50	.9933	.9962
75	.9988	.9988
100	**1.00**	**1.00**
125	.9888	.9888
150	.9977	.9977

All the networks performed similar to each other with a 99% accuracy or above, and there was no clear correlation between hidden layer size and accuracy. The configuration with 100 nodes after training for 109 epochs yielded a 100% accuracy for training, validation, and testing data. This training epoch had a validation performance of .00852 from the CELF. The total confusion matrix can be seen in fig. (4). The column on the far right of the plot shows the precision of each class, or the percentage of the classes that were correctly identified. While the bottom row shows the recall of the examples or the percentage of examples that were correctly identified as positive. The bottom right corner shows the overall accuracy of the ANN, which is equal to the Micro F1 score as discussed in the method.

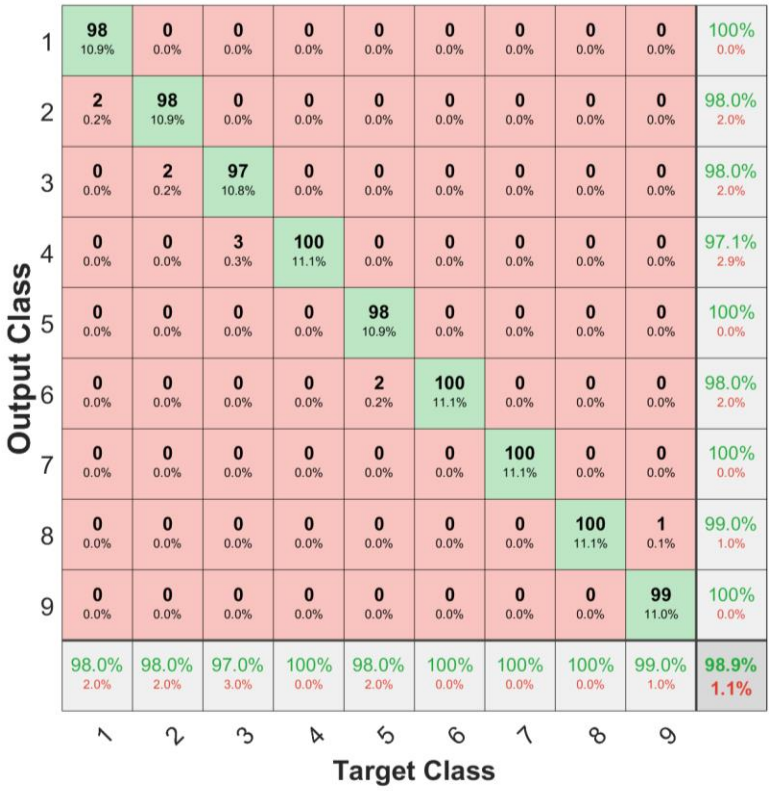

Figure 4: *Total data confusion matrix for 125 node hidden layer size. The green diagonal represents the data sets the network got correct. The far-right column shows the precision for each class, while the bottom row shows the recall.*

3.2 Sensitivity Analysis on ANN:

The last part of the study was to analyze the sensitivity of the network to find the smallest amount of concentration change the network can classify. The hidden layer configuration of 100 nodes was used for each network training, as it showed the highest level of accuracy in the previous section. In order to reduce the output size a 0-10% of glycol concentration was simulated in COMSOL. This data was used to train five different networks: .1%, .2%, .5%, 1%, 2%, and 5% change in the concentration of glycol. It was found that the sensitivity had an inverse effect on the accuracy. It means that as the ANN was trained to classify smaller percent changes in glycol the overall accuracy declined. Along with this, the number of epochs increased as the sensitivity increased. This study shows promise that the ANN can classify small changes in glycol concentrations up to .2%, with a 96.5% accuracy. These results can be seen in fig. (5). The accuracy of the model is comparable to the results found in Kurt's ANN regression model utilizing the Fourier method [20]. One distinct difference is the number of different input types. Kurt's regression model used temperature, nano-particle concentration, and fluid density as inputs to the ANN. Direct comparisons cannot be made to Kurt's regression model as the methods to measure accuracy between regression and classification are different. Where regression utilizes a R^2 and mean average percent error to measure accuracy, and classification utilizes the F1 score. However, our approach could be used as an alternative to Kurt's regression model in which the heat parameters of the fluid such as density and concentration are unknown.

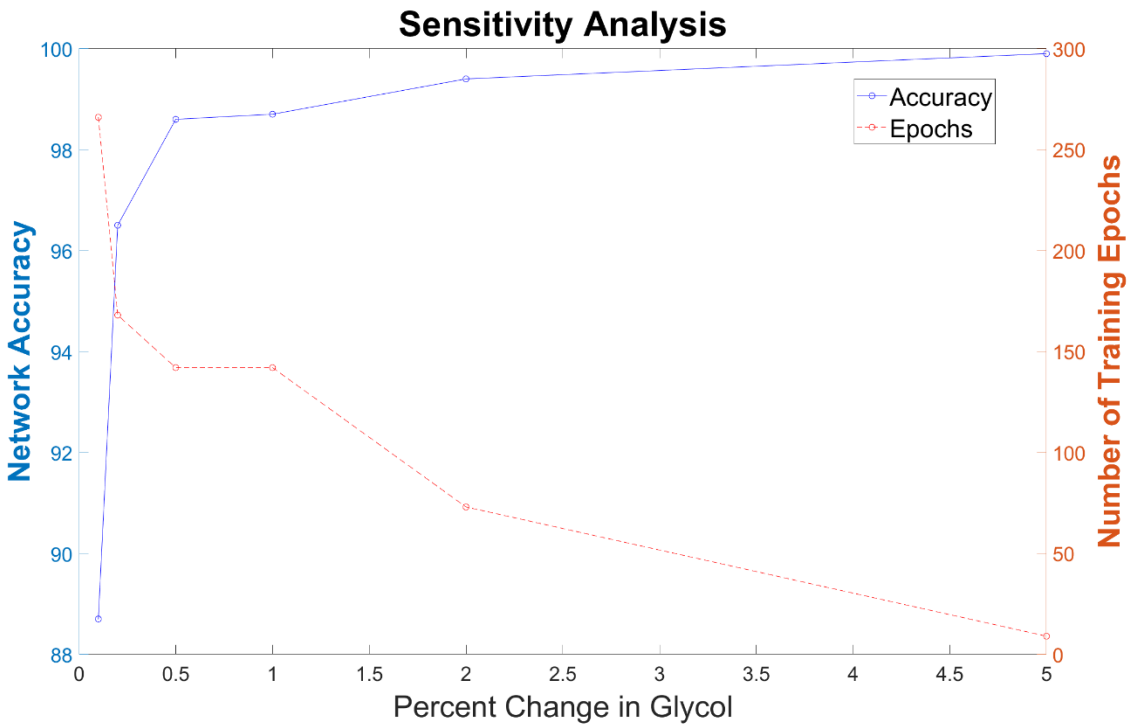

Figure 5: *Sensitivity Analysis of varying percent changes in glycol concentrations. The left axis represents accuracy of the trained ANN, and the right axis represents the number of epochs needed to converge to a minimum error*

4. Conclusion

In the proposed study, it was found that the Artificial Neural Network can accurately classify the thermal conductivity of water-glycol mixtures at various concentrations. Training data were created by COMSOL, a PDE solver. The numerical model to obtain training data for the ANN is an MTS tip in an infinite media subjected to laser irradiation where all parameters were held constant except for the thermal conductivity. The simulation consisted of heating the tip of the MTS with a 500 μs laser pulse at 532 nm wavelength, and the transient temperature profile was collected. MATLAB was used to generate the ANN model and randomize the data sets into training, validation, and testing. Different network arrangements were tested by varying the number of nodes in the hidden layer from 25-150. Training of the network consisted of SCGM. Once the network was trained, validation and test sets were fed into the trained ANN.

The highest accuracy ANN configuration was with a hidden layer of 100 nodes, which attained an overall classification accuracy of 100.00% from training, validation, and test data sets. There was no statistical correlation between the layer size and the accuracy. A sensitivity analysis was also conducted on the ANN and showed a 96.5% accuracy in classifying glycol changes up to 0.2%, or a 0.0066 W/m*K change in thermal conductivity. However, these were only verified with simulated data. To further prove the method, the model must be verified against experimental data. This proposed approach is unique as it uses a classification ANN that is trained with time-series heat propagation data, whereas others use a regression model trained with density, concentration, and current temperature of the sample [19, 20], which is useful for real-time physical and biological property measurements. Applications for this model

are time-critical medical scenarios i.e. surgical operations, in-situ biological screening, or real-time physiological metabolism analysis.

Acknowledgment

This work was supported by National Science Foundation (award number: 1906553).

Nomenclature

L_{CE}	Cross Entropy Loss Function [-]	T_{max}	Max Temperature [K]
ρ	Density [kgm^{-3}]	T_{min}	Min Temperature [K]
Q	Heat input [mW]	c_p	Specific Heat [$Jkg^{-1}K^{-1}$]
FP	False Positive [-]	k	Thermal Conductivity [$Wm^{-2}K^{-1}$]
FN	False Negative [-]	TP	True Positive [-]

References

[1] M. Abdolahad, M. Janmaleki, M. Taghinejad, H. Taghnejad, F. Salehia and S. Mohajerzadeh, "Single-cell resolution diagnosis of cancer cells by carbon nanotube electrical spectroscopy," *Nanoscale,* Vol. 5 no. 8, 3421-3427, 2018.

[2] D.-K. Kang, M. M. Ali, K. Zhang, E. J. Pone and W. Zhao, "Droplet microfluidics for single-molecule and single-cell analysis in cancer research, diagnosis and therapy," *TrAC Trends in Analytical Chemistry,* vol. 58, pp. 145 - 153, 2014.

[3] B. K. Park, N. Yi, J. Park and D. Kim, "Thermal conductivity of single biological cells and relation with cell viability," *Applied Physics Letters,* vol. 102, 203702, 2013.

[4] Byoung Kyoo Park, J. Park, T.-Y. Choi, D. P. Simmons, J. Ha and D. Kim, "Thermal conductivity of biological cells at cellular level and correlation with disease state," *Journal of Applied Physics,* vol. 119, 224701, 2016.

[5] G. M. P. Y. N. e. a. Kucsko, "Nanometre-scale thermometry in a living cell," *Nature,* vol. 500, p. 54–58, 2013.

[6] F. Vetrone, R. Naccache, A. Zamarrón, A. J. d. l. Fuente, F. Sanz-Rodríguez, L. M. Maestro, E. M. Rodriguez, D. Jaque, J. G. Solé and J. A. Capobianco, "Temperature Sensing Using Fluorescent Nanothermometers," *ASC Nano,* vol. 4, no. 6, p. 3254–3258, 2010.

[7] R. Shrestha, R. Atluri, D. P. Simmons, D. S. Kim and T. Y. Choi, "Thermal conductivity of a Jurkat cell measured by a transient laser point heating method," *International Journal of Heat and Mass Transfer,* vol. 160, p. 120161, 2020.

[8] R. Shrestha, R. Atluri, D. P. Simmons, D. S. Kim and T. Y. Choi, "A micro-pipette thermal sensing technique for measuring the thermal conductivity of non-volatile fluids," *Review of*

Scientific Instruments, vol. 89, 114902, 2018.

[9] B. Zhu, X. Zhu, J. Xie, J. Xu and H. Liu, "Heat Transfer Prediction of Supercritical Carbon Dioxide in Vertical Tube Based on Artificial Neural Networks," *Journal of Thermal Science,* vol. 30, p. 1751–1767, 2021.

[10] J.-H. Lee, J. Kang, W. Shim, H.-S. Chung and T.-E. Sung, "Pattern Detection Model Using a Deep Learning Algorithm for Power Data Analysis in Abnormal Conditions," *Electronics,* vol. 9, no. 7, 1140, 2020.

[11] O. I. Abiodun, A. Jantan, A. E. Omolara, K. V. Dada, N. Ab, E. Mohamed and H. Arshad, "State-of-the-art in artificial neural network applications: A survey," *Heilyon,* vol. 4, no. 11, e00938, 2018.

[12] N. Christiansen, P. Voie, O. Winther and J. Høgsberg, "Comparison of Neural Network Error Measures for Simulation of Slender Marine Structures," *Journal of Applied Mathematics,* 2014(4), 1-11, 2014.

[13] M. Najafabadi, F. Villanustre, T. Khoshgoftaar, N. Seliya, R. Wald and E. Muharemagic, "Deep Learning Applications and Challenges in Big Data Analytics," *Journal of Big Data,* vol. 2, no. 1, 1-21, 2015.

[14] S.-C. Wang, "Artificial Neural Network," in *Interdisciplinary Computing in Java Programming*, Boston, Springer, 2003, pp. 81-100.

[15] M. Fauth, F. Wörgötter and C. Tetzlaff, "The Formation of Multi-synaptic Connections by the Interaction of Synaptic and Structural Plasticity and Their Functional Consequences," *PLOS Computational Biology,* Vol. 11 (1), e1004031, 2015.

[16] L. Huang, J. Qin, Y. Zhou, L. Liu and L. Shao, "Normalization Techniques in Training DNNs: Methodology, Analysis and Application," arXiv Cornell University, 1-20, 2020.

[17] Chai Meijuan, "Application of ANN technique to predict the thermal conductivity of nanofluids: a review," Journal of Thermal Analysis and Calorimetry, 145, 2021-2032 (2021).

[18] Yunmin Liang, Zhichun Liu, and Wei Liu, "A co-training style semi-supervised artificial neural network modeling and its application in thermal conductivity prediction of polymeric composites filled with BN sheets," Energy and AI, Vol. 4, 100052 (2021)

[19] P. Sharma, K. Ramesh, R. Parameshwaran and S. S. Deshmukh, "Thermal conductivity prediction of titania-water nanofluid: A case study using different machine learning algorithms," *Case Studies in Thermal Engineering,* vol. 30, 2022.

[20] H. Kurt and M. Kayfeci, "Prediction of thermal conductivity of ethylene glycol–water solutions by using artificial neural networks," *Applied Energy,* vol. 86, no. 10, pp. 2244-2248, 2009.

[21] Bokai Liu, Nam Vu-Bac, Xiaoying Zhuang, Xiaolong Fu, Timon Rabczuk, “Stochastic integrated machine learning based multiscale approach for the prediction of the thermal conductivity in carbon nanotube reinforced polymeric composites,” Composites Science and Technology, Vol. 224, 109425 (2022).

[22] Shyam S. Sablani, Oon-Doo Baik, Michele Marcotte, “Neural networks for predicting thermal conductivity of bakery products,” Journal of Food Engineering, Vol. 52 (3), 299-304 (2002).

[23] Navid Kardani, Abidhan Bardhan, Pijush Samui, Majidreza Nazem, Panagiotis G. Asteris, Annan Zhou, “Predicting the thermal conductivity of soils using integrated approach of ANN and PSO with adaptive and time-varying acceleration coefficients,” International Journal of Thermal Sciences, Vol. 173, 107427 (2022).

[24] Mohamed Azlan Hussain and M. Shafiur Rahman, “Thermal conductivity prediction of fruits and vegetables using neural networks,” International Journal of Food Properties, Vol. 2, 121-137 (2009).

[25] Manoj Khandelwal, “Prediction of thermal conductivity of rocks by soft computing,” International Journal of Earth Sciences, Vol. 100, 1383-1389 (2011).

[26] Farzad Jaliliantabar, “Thermal conductivity prediction of nano enhanced phase change materials: A comparative machine learning approach,” Journal of Energy Storage, Vol. 46, 103633 (2021).

[27] O. Schenk and K. Gärtner, "PARDISO," in *Encyclopedia of Parallel Computing*, Boston, Springer, 2011, p. 1458–1464.

[28] K. Murphy, Machine Learning, Cambridge: MIT, A Probabilistic Perspective.

[29] L. Bottou, "Large-Scale Machine Learning with Stochastic Gradient Descent," in *COMPSTAT*, Paris, 2010.

[30] I. Markoulidakis, I. Rallis, I. Georgoulas, G. Kopsiaftis, A. Doulamis and N. Doulamis, "Multiclass Confusion Matrix Reduction Method and Its Application on Net Promoter Score Classification Problem," *The 14th Pervasive Technologiies Related to Assistive Environments Conference*, vol. 9, no. 81, 412-419, 2021.

Submitted: 11.03.2022

Revised: 21.06.2022.

Accepted: 12.10.2022.